

ON EFFICIENT QUANTIZATION FOR IMAGE RECOMPRESSION

Ora Gendler and Moshe Porat

Department of Electrical Engineering, Technion - Israel Institute of Technology
Haifa 32000, Israel

phone: +972-4-8294684, fax: +972-4-8295757, email: orag@tx.technion.ac.il, mp@ee.technion.ac.il

ABSTRACT

It is well known that both the rate and the distortion of re-compressed images depend primarily on the ratio between the new and the old quantization steps used. In this paper we provide a theoretical basis to this observation, and introduce an efficient algorithm to select the recompression quantization step. Our approach is based on the structure of the quantizer and the distribution of DCT coefficients in subband coding. These results can be readily generalized to re-quantization of other data types. Our conclusion is that the proposed approach could be instrumental in recompression of still images, while offering straightforward generalization to higher and lower dimension signals.

1. INTRODUCTION

Many visual applications involve storage and transmission of coded images. Often, the data to be transmitted is initially coded and stored in high quality. Later on, when transmission is required, in many cases, the bit-rate of the data has to be reduced, to meet the limitations of the transmission media and the available resources at the receiving end.

An overview of various bit-rate reduction methods, namely recompression or transcoding, can be found in [1]. Most applications require that the method be fast and simple while keeping the distortion as low as possible. These demands rule out intuitive solutions such as a cascaded encoder-decoder, which are neither fast nor necessarily optimal.

The focus of this work is on bit-rate reduction of coded images, by means of uniform re-quantization. This approach involves quantization in two stages. The first stage of quantization is performed at the encoder and cannot be controlled, altered or avoided. The second stage of quantization is performed for recompression. This work deals with designing the second stage quantizer of previously quantized data for bit-rate reduction. The obtained quantizer design is a result of theoretical rate-distortion analysis, carried out throughout all re-quantization stages. Moreover, though applied here to coded images in the transform domain, the analysis could be used for other data types as well such as 1D signals (e.g., audio) as well as 3D signals, like 3D imaging or video.

This work is organized as follows. Section 2 introduces the required definitions for the rate-distortion analysis carried out in Section 3. In Section 4 experimental results are presented and in Section 5 this work is concluded.

2. PROBLEM DEFINITION

Consider a basic image coding scheme where DCT is applied to each image block. Each DCT coefficient $x_{u,v}$ at position (u,v) in the image is then quantized and the image is coded using variable length coding (VLC). Then, a basic re-quantization scheme is applied. The coded image is decoded (VLD), re-quantized in the DCT domain and encoded again (VLC). The first stage quantizer is denoted by Q_1 and the quantization step size used is q_1 . The second stage quantizer is denoted by Q_2 and the quantization step size used is q_2 . In addition, a third reference quantizer is used throughout this work denoted by $Q_{2,ref}$. The reference coarse quantizer is used directly on the original signal, referred to as *direct quantization*. $Q_{2,ref}$ is mainly used to evaluate the performance of the second stage quantizer.

A uniform threshold quantizer (UTQ or midtread) is used for all quantization stages, as in [2] and [3]. The quantization is uniform, i.e., all the DCT coefficients in the image are quantized using the same quantization step. The quantizer is shown in Fig. 1 and defined by:

$$\begin{aligned} Q_1(x_{u,v}) &= \text{Round}(x_{u,v} / q_1 + 0.5) \\ Q_1^{-1}(x_{u,v}) &= Q_1(x_{u,v}) \cdot q_1 \\ Q_2(x_{u,v}) &= \text{Round}(Q_1^{-1}(Q_1(x_{u,v})) / q_2 + 0.5) \\ Q_{2,ref}(x_{u,v}) &= \text{Round}(x_{u,v} / q_2 + 0.5) \end{aligned} \quad (1)$$

The decision and reconstruction levels of the UTQ are defined as:

$$d_{i,0} = 0; \quad d_{i,j} = (j - 0.5)q_i; \quad r_{i,0} = 0; \quad r_{i,j} = j \cdot q_i, \quad (2)$$

where $d_{i,j}$ is decision level j of the stage i ($i=1,2$) quantizer and $r_{i,j}$ is the reconstruction level.

The rounding operation in the second stage quantization could be carried out in two ways that differ by how 0.5 is rounded. One option is to round 0.5 to 1 and the other is to round it toward 0. It was shown in [4] that rounding to 0 improves the re-quantization performance substantially and that is the rounding method used in this work.

The main goal of this work is to design the second stage quantizer used for image re-quantization so that the bit reduction is performed effectively with little distortion. Thus, we

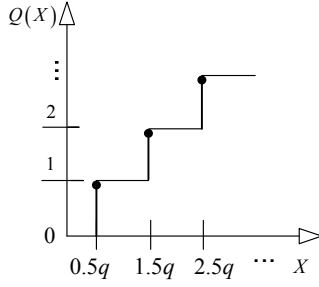


Figure 1: UTQ quantizer illustration

aim to avoid distortion introduced by quantization in two stages instead of using one coarse quantizer, i.e.:

$$\forall x, u, v : Q_2(x_{u,v}) = Q_{2,ref}(x_{u,v}) . \quad (3)$$

To do so, the new re-quantization step size must be a multiple of the first stage quantization step size [2] [3] [5] so that:

$$q_2 = kq_1, \quad k \in \mathbb{N} . \quad (4)$$

Choosing q_2 according to the requirement in (4) allows developing rate and distortion expressions for the re-quantized DCT coefficients, as a function of k . The resulting rate-distortion analysis is used to design and evaluate the second stage quantizer; it is presented below.

3. RATE-DISTORTION ANALYSIS

Analysis of the distortion and bit-rate of re-quantized images in the transform domain requires modelling the probability distribution of the DCT coefficients throughout all stages of quantization. The distribution of the DCT coefficients of images is assumed to be Laplace [6], defined by:

$$p(x) = 0.5\lambda e^{-\lambda|x|} . \quad (5)$$

The bit-rate and distortion analysis that follows can be easily generalized to other data types of one-, two- and three-dimensions. The indices (u,v) denoting the position of the DCT coefficient in the image can be replaced with 1D or 3D notations, respectively, and the re-quantization of 1D signal samples or 3D voxels could be analyzed similarly. The only additional information needed is on the PDF (probability density function) of the DCT coefficient $x_{u,v}$ and on the structure of the UTQ used. In the rest of the paper, the indices are therefore omitted for convenience.

3.1 Bit-rate Analysis

The bit-rate of the re-quantized image coefficients is estimated using the entropy, defined by

$$H = - \sum_{j=-\infty}^{\infty} p(r_{2,j}) \log_2 p(r_{2,j}) , \quad (6)$$

where $r_{2,j}$ is the representation level of quantization bin j of the second stage quantizer.

First, to estimate the PMF (Probability Mass Function) of the DCT coefficients after first stage quantization, the probability weights of each quantization bin of the first stage

quantizer are calculated. For quantization step q and positive values (symmetrical for the negative values), the probability weight w_j of bin j of the first stage quantizer is expressed as:

$$w_j = 0.5\lambda \int_{(j-0.5)q}^{(j+0.5)q} e^{-\lambda x} dx = 0.5e^{-\lambda(j-0.5)q} (1 - e^{-\lambda q}) . \quad (7)$$

Thus, when calculating the PMF of the visual data after first stage quantization, each possible value is a reconstruction level of a quantization bin from the first stage quantizer with probability weight accordingly. Similarly, the distribution of re-quantized data (after second stage quantization) also consists of probability weights of the quantizer's representation levels. In fact, it is possible to regard the re-quantization process as *rearranging of the probability weights* (of quantized coefficients) into new groups, representing the re-quantized values and their probability distribution. The probability weights of the re-quantized data are determined by the position of the decision levels of the second stage quantizer $d_{2,m}$ relative to the decision levels of the first stage quantizer $d_{1,j}$.

The entropy of data re-quantized with Q_2 and $Q_{2,ref}$ was derived as a function of the integer factor k , as defined in (4). Note that for odd values of k both the rate and the distortion performance of Q_2 and $Q_{2,ref}$ is the same. This happens because when k is odd, all decision levels of the second stage quantizer coincide with some decision levels of the first stage quantizer, as shown in (8) below and in more detail in [4].

$$\begin{aligned} (*) \quad q_2 = kq_1 = \{k \text{ odd}\} &= (2s+1)q_1 \\ d_{2,m} = (m-0.5)q_2 &= \underbrace{(m(2s+1)-s)}_l q_1 - 0.5q_1 = d_{1,l} \quad (8) \\ \Rightarrow \forall m \exists l : d_{2,m} &= d_{1,l} \end{aligned}$$

The entropy expressions were derived separately for odd and even values of k . The expression for entropy (measured in bits/pixel) are shown in Table 1 and plotted in Fig. 2, as a function of k . The first stage quantization step size used for the plot is $q_1 = 10$ and the parameter λ is set to 0.1, a suitable value for typical images [6].

It can be seen that for re-quantization, a much steeper decrease in entropy occurs when k is even. This shows that better compression can be achieved at these points. This happens due to the position of second stage decision levels relative to first stage decision levels in a way that causes more probability weights to merge together as a result of re-quantization. This drastically decreases the entropy.

When comparing to the direct quantization curve, it can be observed that for the even k values, the entropy is smaller for re-quantization. At the odd values, as expected, the entropy of the re-quantized data is equal to that of the data quantized once with the coarse reference quantizer.

These entropy expressions allow estimating the bit rate of the re-quantized image for various values of q_2 , without actually performing the re-quantization repeatedly.

k	$E[\text{bits/pixel}]$
Odd	$\lambda \cdot \int_0^{0.5kq_1} e^{-\lambda x} dx \cdot \text{Log}_2 \left(0.5\lambda \cdot \int_0^{0.5kq_1} e^{-\lambda x} dx \right) + \lambda \cdot \sum_{l=1}^{\infty} \left[\int_{k(l-0.5)q_1}^{k(l+0.5)q_1} e^{-\lambda x} dx \cdot \text{Log}_2 \left(0.5\lambda \cdot \int_{k(l-0.5)q_1}^{k(l+0.5)q_1} e^{-\lambda x} dx \right) \right] =$ $e^{-0.5k\lambda q_1} \left(-k\lambda q_1 e^{k\lambda q_1} + e^{1.5k\lambda q_1} \ln \left[0.5(1 - e^{-0.5k\lambda q_1}) \right] + \right. \\ \left. + (e^{k\lambda q_1} - 1) \ln \left[1 + e^{0.5k\lambda q_1} \right] + e^{0.5k\lambda q_1} \ln \left[1 + \text{Coth}(0.25k\lambda q_1) \right] \right) / (e^{k\lambda q_1} - 1) \ln(2)$
Even	$\lambda \int_0^{0.5(k+1)q_1} e^{-\lambda x} dx \cdot \text{Log}_2 \left(\frac{\lambda}{2} \int_0^{0.5(k+1)q_1} e^{-\lambda x} dx \right) + \lambda \sum_{l=1}^{\infty} \left[\int_{(kl-0.5(k-1))q_1}^{(kl+0.5(k+1))q_1} e^{-\lambda x} dx \cdot \text{Log}_2 \left(\frac{\lambda}{2} \int_{(kl-0.5(k-1))q_1}^{(kl+0.5(k+1))q_1} e^{-\lambda x} dx \right) \right] =$ $= \left(2 \ln \left[\frac{1}{2} - \frac{e^{-0.5(k+1)\lambda q_1}}{2} \right] - e^{-0.5(k+1)\lambda q_1} \cdot \left((2k+1)\lambda q_1 + k\lambda q_1 \text{Coth}[0.5k\lambda q_1] + 2 \ln \left[\frac{1 - e^{-0.5(k+1)\lambda q_1}}{e^{k\lambda q_1} - 1} \right] \right) \right) / \ln(4)$

Table 1: Entropy of re-quantized Laplace PDF

k	D
Odd	$\lambda \int_0^{0.5kq_1} x^2 e^{-\lambda x} dx + \sum_{l=1}^{\infty} \left[\lambda \int_{k(l-0.5)q_1}^{k(l+0.5)q_1} (x - klq_1)^2 e^{-\lambda x} dx \right] = \frac{2 - k\lambda q_1 \text{Csch}[0.5k\lambda q_1]}{\lambda^2}$
Even	$\lambda \int_0^{0.5(k+1)q_1} x^2 e^{-\lambda x} dx + \sum_{l=1}^{\infty} \left[\lambda \int_{0.5(2kl-k+1)q_1}^{0.5(2kl+k+1)q_1} (x - klq_1)^2 e^{-\lambda x} dx \right] = (e^{k\lambda q_1} - 0.5k\lambda q_1 (2 + \lambda q_1) e^{0.5(k-1)\lambda q_1} - 1) \cdot$ $\cdot (\text{Coth}[0.5k\lambda q_1] - 1) / \lambda^2$

Table 2: Distortion of re-quantized Laplace PDF

3.2 Distortion Analysis

The distortion of re-quantized DCT coefficients is based on the Laplace distribution in (5) and is defined as:

$$D = 0.5\lambda \int_{-\infty}^{\infty} (x - \hat{x})^2 e^{-\lambda|x|} dx =$$

$$= \lambda \int_0^{d_{2,1}} x^2 e^{-\lambda x} dx + \lambda \sum_{j=1}^{\infty} \int_{d_{2,j}}^{d_{2,j+1}} (x - r_{2,j})^2 e^{-\lambda x} dx \quad (9)$$

The distortion is evaluated as a function of k , separately for odd and even values. As before, for odd values of k , the distortion for re-quantization and direct quantization is the same. Distortion expressions appear in Table 2 and are plotted in Fig. 3, as a function of k . Once again, $q_1 = 10$ and $\lambda = 0.1$. It can be observed that for re-quantization, a much steeper increase in distortion occurs when k is even and at these points it is higher than the distortion of the direct quantizer. This means that when re-quantizing with an even multiple of the original quantization step, additional distortion (comparing to direct quantization) is inevitable, whereas for the odd multiples, both re-quantization and direct quantization cause the same distortion. In addition, as k increases, the distortion for re-quantization and direct quantization converges to the same value. This is caused by the growing probability weight of the zero quantization bin $[-0.5kq_1, 0.5kq_1]$, which increases according to:

$$P_{\text{zero-bin}} = 0.5\lambda \int_{-kq_1/2}^{kq_1/2} e^{-\lambda|x|} dx = \{q_1 = 10\} = 1 - e^{-5\lambda k} \quad (10)$$

Since this bin is quantized to zero in both cases, when $P_{\text{zero-bin}} \approx 1$, the distortion for direct quantization and re-quantization converges to the same value. It can be easily shown that for $k > 10$, $P_{\text{zero-bin}} \approx 1$, which explains the close values in Fig. 3, for both methods. Similar behaviour can be observed in Fig. 2, for the entropy.

3.3 Rate-Distortion Functions

The developed rate and distortion expressions are used to analyze the performance of the second stage quantizer. Fig. 4 shows rate vs. distortion. It can be seen that re-quantization performs better than direct quantization at some areas of the curve. In addition, there are areas of the re-quantization curve where moving towards substantially higher distortion does not substantially reduce the rate. For instance, when moving right from $D \approx 85$ to $D \approx 100$, the rate remains $R \approx 1.3$ bit per pixel. This means that there are some re-quantization step sizes that will cause a larger distortion without reducing the rate. Clearly such re-quantization steps are best avoided. Experimental results validating these notions are presented next.

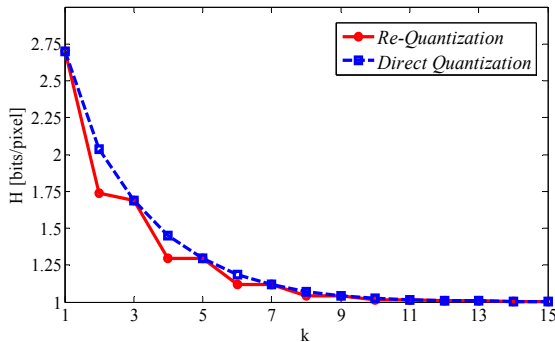


Figure 2: Theoretical entropy of requantized Laplace PDF initially quantized with $q_1 = 10$, as a function of $k = q_2/q_1$, for re-quantization and for direct quantization.

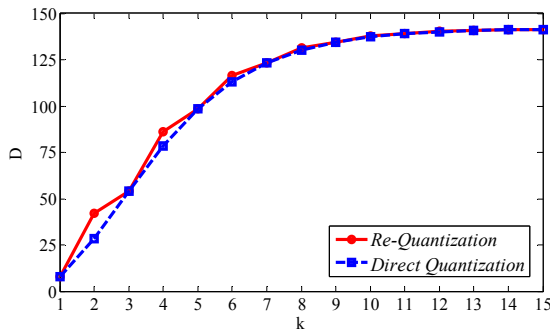


Figure 3: Theoretical distortion of re-quantized Laplace PDF originally quantized with $q_1 = 10$, as a function of $k = q_2/q_1$ for re-quantization and for direct quantization.

4. EXPERIMENTAL RESULTS

Simulations were conducted on typical images, using various q_1 and q_2 . The 'Man' image presented in Fig. 5 (top) was initially quantized with $q_1=15$ and then re-quantized. The middle image shows 'Man' after re-quantization with $q_2=29$ and the bottom image in Fig. 5 shows 'Man' after re-quantization with a slightly coarser re-quantization step of $q_2=30=2 \cdot q_1$. It can be easily observed that the bottom image in Fig. 5 ($q_2=30$) looks much better than the middle one ($q_2=29$). There is less noise and the uniform areas of the image appear to be much smoother. Also quantitatively, despite the coarser re-quantization step used in the bottom image, its PSNR is higher by approximately 1.5 dB. Moreover, the compression ratio of the image re-quantized with $q_2=30$ is much higher than the compression ratio of the image re-quantized with $q_2=29$ (note that the bit-rate is more than two times lower). This behavior can also be observed in Fig. 6, showing the rate as function of q_2 , for initial quantization with $q_1 = 10$. Obviously, at even multiples of the original quantization step, the rate decreases dramatically, as theoretically observed in 3.1. Fig. 7 shows the distortion (MSE) as a function of q_2 . It can be observed that the local minimum is at odd multiples (when $q_2=30=3 \cdot q_1$ and $q_2=50=5 \cdot q_1$). However, the maximal distortion is achieved one step before the even multiples, which allows using the even multiples at relatively low distortion. This is due to the rounding method used [4].

Fig. 8 shows empirical rate-distortion for both direct quantization and re-quantization, averaged for 7 different images,

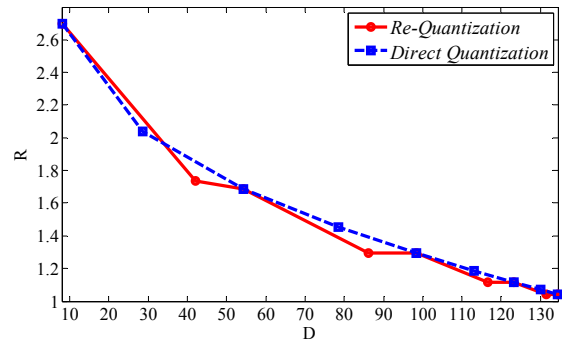


Figure 4: Theoretical rate vs. distortion for re-quantized Laplace PDF, initially quantized with $q_1 = 10$. As can be seen, there are points where re-quantization outperforms direct quantization and intervals where the slopes of the curve change significantly.

using $q_1 = 10$ and $\lambda = 0.1$, as in the theoretical analysis. The behaviour of the curves is quite similar to the theoretical. Clearly there are intervals where re-quantization outperforms direct quantization (this happens at the even values of k) and there are undesired re-quantization steps that increase distortion without decreasing the rate significantly.

5. CONCLUSIONS

A re-quantization method for recompression of images in the DCT domain has been analyzed from a rate-distortion point of view. The process of re-quantization involves selection of the second stage quantization step. To avoid added distortion due to re-quantization, it is proposed to select the re-quantization step as an even multiple of the original quantization step [2], [3].

The efficiency and the performance of the proposed method have been evaluated based on the obtained bit-rate, MSE and the visual quality of the recompressed images. We have shown in our theoretical analysis that the bit-rate of the re-quantized image decreases significantly when the re-quantization step is an even multiple of the original step size.

On the other hand, the MSE is minimized at odd multiples of the original quantization step size and increases at even multiples. However the visual quality obtained at even multiples is still much better than for other (not integer multiples of original quantization step) re-quantization steps.

This work has introduced a rate-distortion function for image re-quantization. Even though developed for the Laplace distribution of the DCT coefficients of 2D images and the midtread quantizer, this work could be readily generalized to other dimensions [7]. For 2D images, our conclusion is that the most efficient re-quantization is achieved by selecting the re-quantization step as an even multiple of the original quantization step and rounding the re-quantized coefficients towards zero. The rate and distortion of the re-quantized image could be estimated offline, thus improving currently available recompression systems, including real-time applications.

ACKNOWLEDGEMENT This work was supported in part by the Ollendorff Minerva Centre. Minerva is funded through the BMBF.

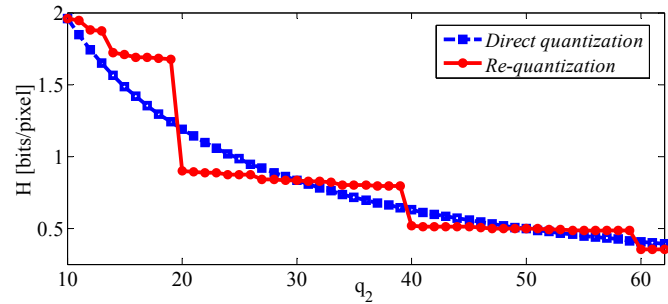
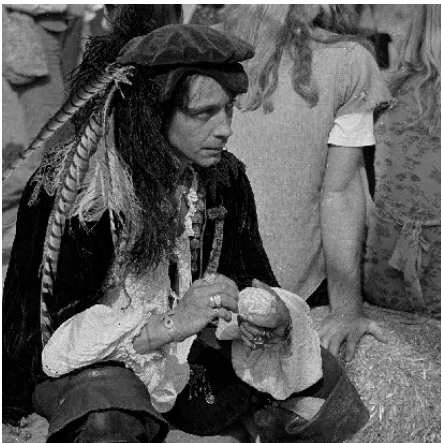


Figure 6: Rate as a function of uniform re-quantization step q_2 , for $q_1=10$, averaged for 7 images. Note the substantial rate decrease at $q_2=2\cdot q_1=20$ and $q_2=4\cdot q_1=40$, i.e., at even multiples, according to the theoretical analysis.

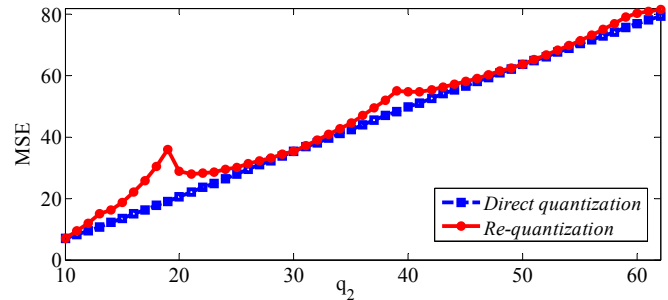


Figure 7: MSE as a function of q_2 , for $q_1=10$, averaged for 7 re-quantized images. Note that MSE is equal for both methods at $q_2=30$ and $q_2=50$, also there is significant added distortion due to re-quantization at $q_2=20, 40$ and 60 . Still, the local distortion peaks occur at $q_2=19, 39$ and 59 .

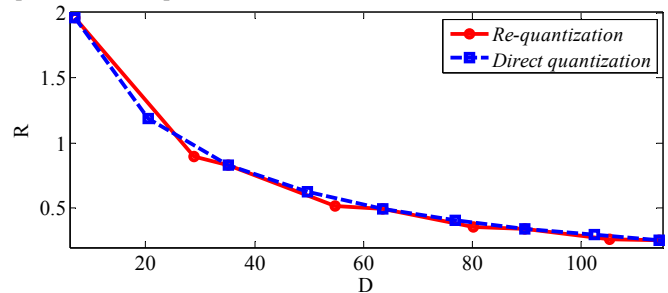


Figure 8: Rate vs. distortion, averaged for 7 re-quantized images, after initial uniform quantization with $q_1=10$. Rate-distortion behaviour is similar to that of theoretic rate-distortion shown in Fig. 4.

Figure 5 (on the left): The 'Man' image, initially quantized with $q_1=15$, then re-quantized. Top: Original image. Middle: Re-quantized with $q_2=29$, obtaining PSNR of 30.54dB, at 1.18 bit/ pixel. Bottom: Re-quantized with $q_2=30$, with PSNR= 32.1 dB, at 0.54 bit/pixel. As can be seen, the bottom image outperforms the middle one, both visually and quantitatively.

6. REFERENCES

- [1] I. Ahmad, X. Wei, Y. Sun and Y.Q. Zhang, "Video Transcoding: An Overview of Various Techniques and Research Issues", *IEEE Trans. on Multimedia*, Vol. 7, pp. 793-804, Oct. 2005.
- [2] A. Leventer and M. Porat, "Towards optimal bit-rate control in video transcoding", *the IEEE International Conference on Image Processing*, Vol. 3, pp.265-8, Sep. 2003.
- [3] O. Werner, "Requantization for transcoding of MPEG-2 Intraframes," *IEEE Trans. on Image Processing*, Vol. 8, No. 2, pp.179-191, Feb. 1999.
- [4] O. Gendler, M.Porat, "On transcoding optimization using requantization" CCIT Report No. 717, Technion, Jan. 2009.
- [5] H.H Bauschke, C.H.Hamilton, M.S Macklem, J.S McMichael, and N.R Swart, "Recompression of JPEG Images by Requantization", *IEEE Trans. on Image Processing*, Vol. 12, Issue 7, pp. 843 - 849 , July 2003
- [6] S. R. Smoot, L. A. Rowe, and E.F. Roberts, "Laplacian model for AC DCT terms in image and video coding," *Proc. of the International Workshop on Network and Operating Systems Support for Digital Audio and Video*, pp.60-9, 2003.
- [7] A. Francos and M. Porat, "Analysis and Synthesis of Multicomponent Signals using Positive Time-Frequency Distributions", *IEEE Trans. on Signal Processing*, Vol. 47, No. 2, pp. 493-504, 1999.